Advances in Materials Research, *Vol. 13, No. 1 (2024) 55-62*
https://doi.org/10.12989/amr.2024.13.1.055

The synthesis and properties of point defect structure of $Cu_{2-x}ZnSnS_4$ (x=0.1, 0.2, and 0.3)

Bui D. Long* and Le T. Bang[a]

School of Materials Science and Engineering, Hanoi University of Science and Technology, No.1 Dai Co Viet, Hai Ba Trung, Hanoi, Vietnam

(*Received September 7, 2021, Revised April 17, 2023, Accepted July 21, 2023*)

Abstract. Cu-based sulfides have recently emerged as promising thermoelectric (TE) materials due to their low cost, non-toxicity, and abundance. In this research, point defect structure of $Cu_{2-x}ZnSnS_4$ (x=0.1, 0.2, 0.3) samples were synthesized by the mechanical alloying method. Mixed powders of Cu, Zn, Sn and S were milled using high energy ball milling at a rotation speed of 300 rpm in Ar atmosphere. The milled $Cu_{2-x}ZnSnS_4$ powders were heat-treated at 723 K for 24 h, and subsequently consolidated using spark plasma sintering (SPS) under an applied pressure of 60 MPa for 15 min. The thermal conductivity of the sintered $Cu_{2-x}ZnSnS_4$ samples was evaluated. A well-defined $Cu_{2-x}ZnSnS_4$ powders were successfully formed after milling for 16 h, with the particle sizes mostly distributed in the range of 60-100 nm. The lattice constants of *a* and *c* decreased with increasing composition value *x*. The thermal conductivity of sintered x=0.1 sample exhibited the lowest value and attained 0.93 W/m K at 673 K.

Keywords: Cu_2ZnSnS_4; mechanical alloying and thermal conductivity; thermoelectric materials

1. Introduction

The Seebeck effect was discovered by Thomas Johann Seebeck in 1821, in which a voltage different (ΔV) will form when a temperature differential (ΔT) is imposed on a thermoelectric (TE) junction of two dissimilar metals (Row 2012, Fitriani *et al.* 2016, Ge *et al.* 2016). The magnitude of ΔV is proportional to the ΔT, whilst the ratio of the induced voltage to the temperature difference ($\Delta V/\Delta T$) is denoted as the Seebeck coefficient (S), or the thermopower. The performance of TE materials can be expressed by the Figure of merit (ZT)

$$ZT = \frac{S^2\sigma}{\kappa}T \tag{1}$$

where σ, κ, and T are the electrical conductivity, thermal conductivity, and the absolute temperature at which the properties are measured, respectively. High performance TE materials require high ZT values, which need high power factor, $S^2\sigma$, and low κ.

The thermoelectric generators (TEGs), composing from *p*- and *n*- type TE materials without moving parts, are capable of generating power outputs from microwatts to hundreds kW, and

*Corresponding author, Ph.D., E-mail: long.buiduc@hust.edu.vn
[a]Ph.D.

potentially to MW (Freer and Powell 2020). In fact, TEGs can be used to directly convert the waste heat from metallurgy, electronic device industries, solid-wastes burning, automobile exhaust, resident heating etc. into usable electricity. Thus, TE technology can significantly contribute to the improvement of energy consumption efficiency, the reduction of greenhouse gas emissions, and providing cleaner forms of energy (Jaziri *et al.* 2020).

Despite having a relatively large bandgap, E_g~1.5 eV, the *p*-type semiconductor Cu_2ZnSnS_4 quaternary chalcogenide has attracted attention as a promising candidate for TE applications due to its intrinsically low thermal conductivity, κ~1 W m^{-1} K^{-1} at 700 K, coupled with the complex structure, which can be used to tune transport properties. In addition, Cu_2ZnSnS_4 contains low cost, environmentally favorable elements (Long *et al.* 2021, Kosuga *et al.* 2015). However, Cu_2ZnSnS_4 is an intrinsic semiconductor with a very low ZT value of 0.039 at 700 K (Liu *et al.* 2009).

In order to improve the performance of Cu_2ZnSnS_4, the first attempt to interfere in the structure and chemical composition of Cu_2ZnSnS_4 as $Cu_{2+x}Zn_{1-x}SnS_4$ (x=0, 0.1) was conducted by Liu *et al.* (2009). In this research, the performance of $Cu_{2+x}Zn_{1-x}SnS_4$ was significantly enhanced by a partial substitution (x=0.1) of Cu for Zn doped hole carriers into the valence band, leading to an enhancement of σ to 1.31×10^4 S m^{-1}. Furthermore, the substitution also decreased the thermal conductivity κ from 1.21 W K^{-1} m^{-1} to 1.12 W K^{-1} m^{-1} at 700 K, which led to the increase of *ZT* value to 0.36 at 700 K. After Liu *et al.* (2009), efforts have been devoted for the synthesis and improving the performance of Cu_2ZnSnS_4 by doping method (Yang *et al.* 2012, Long *et al.* 2019, Jiang *et al.* 2020, Long *et al.* 2021). Recently, Nagaoka *et al.* (2018) conducted another route to improve the *ZT* value of Cu_2ZnSnS_4 by synthesizing a Cu poor sample with the Cu, Zn, Sn and S ratio of 1.8:1.05:0.95:4. The results showed that the σ of $Cu_{1.8}Zn_{1.05}Sn_{0.94}$ was significantly improved, whilst the κ was decreased compared to that of stoichiometric composition, subsequentially led to the increase of *ZT* value to 0.2 at 400 K. There is still room to improve the *ZT* value of Cu_2ZnSnS_4 by further tuning the chemical composition and crystal structure (e.g., by reducing the Cu atomic ratio to 1.7).

Thus, in this research, we attempted to further improve the performance of Cu_2ZnSnS_4 by reducing the thermal conductivity through the creation of large point defects of the Cu sites in the crystal structure as $Cu_{2-x}ZnSnS_4$ (x=0.1, 0.2, 0.3). The mechanical alloying was chosen as the synthesis method because it is simple and able to synthesize a homogeneous composition, ultra-fine powder particles, and solving the vapor problem of S. The phase formation and morphology of milled $Cu_{2-x}ZnSnS_4$ powders were characterized. The effects of x on the lattice constants and the thermal conductivity were investigated.

2. Materials and method

2.1 Materials

Cu (99.5%, -100 mesh, Strem Chemicals), Zn (99.9%, -325 mesh, Strem Chemicals), Sn (99.5%, -100 mesh, Alfa Aesar), and S (99.5%, -325 mesh, Alfa Aesar) powders were used as raw materials without purification.

2.2 Methods

The mixtures of Cu, Zn, Sn, and S powders were prepared with different compositions of Cu_{2-}

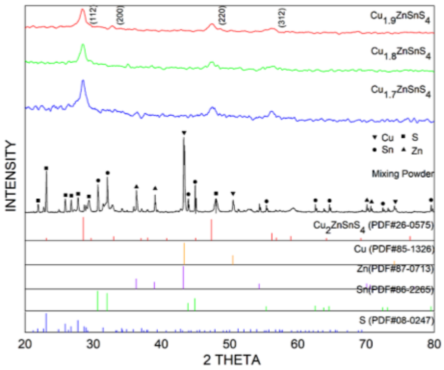

Fig. 1 XRD patterns of the mixture of Cu, Zn, Sn, and S powders of $Cu_{2-x}ZnSnS_4$ (x=0.1, 0.2, 0.3) samples before and after milling for 16 h

$_x$ZnSnS$_4$ (x=0.1, 0.2, 0.3) samples. The mixed powders were milled for 16 h in a high-purity Ar atmosphere using a Fritsch Planetary Mono Mill Pulverisette 6. The balls to powder ratio and milling speed were of 10:1 and 300 rpm, respectively. In order to avoid contamination from the grinding media, a zirconia container and balls were used. After milling, the milled $Cu_{2-x}ZnSnS_4$ powders were heat-treated using a muffle furnace (Nabertherm B150) at a temperature of 723 K for 24 h in Ar atmosphere. The heat-treated $Cu_{2-x}ZnSnS_4$ powders were then sintered by SPS at 873 K under an applied pressure of 60 MPa for 15 min. The relative densities of the sintered samples were determined from their weight and dimensions, which gave a high value of ~97%.

2.3 Characterization

The phase formation of the mixed powders after ball milling and heat treatment were analyzed by X-ray diffraction (XRD) using a Bruker D8 Advance diffractometer with Cu K_α radiation (1.54059 Å). The surface morphologies of the milled $Cu_{2-x}ZnSnS_4$ powders were characterized by field emission-scanning electron microscopy (FE-SEM, Hitachi S4800). For particle size distribution analysis, random 50 particles from each image were measured using ImageJ software. The attice constants, a and c, was measured by high-scoreX'pert software based on XRD data, which includes peak position, Miller index (hkl), and interspacing d.

The thermal diffusivity (α) and specific heat (C_p) were also simultaneously measured on a plate-shaped specimen (5×5×0.5 mm) using a commercial laser flash thermal measurement apparatus (LFA-502, Kyoto Electronics) in the temperature range of 300-673 K. The obtained data were used to calculate the thermal conductivity as $\kappa=\alpha C_p d_s$, where d_s is the density of the sample.

3. Results and discussion

3.1 Formation of the milled $Cu_{2-x}ZnSnS_4$ powders

XRD patterns of the mixtures of Cu, Zn, Sn, and S of $Cu_{2-x}ZnSnS_4$ (x=0.1, 0.2, 0.3) powders before and after milling are shown in Fig. 1. Peaks of Cu, Zn, Sn, and S powders were present in the XRD pattern of the mixed powder. However, the XRD peaks of single elements disappeared after

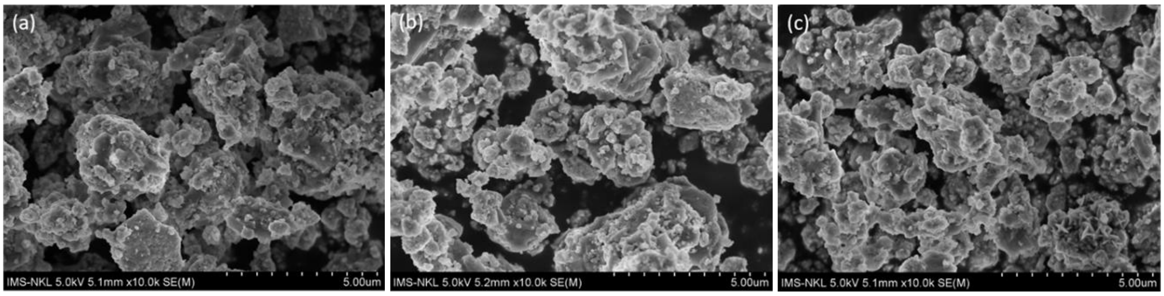

(a) x=0.1 (b) x=0.2 (c) x=0.3

Fig. 2 Morphologies of the as-milled $Cu_{2-x}ZnSnS_4$ powders after milling for 16 h with different compositions

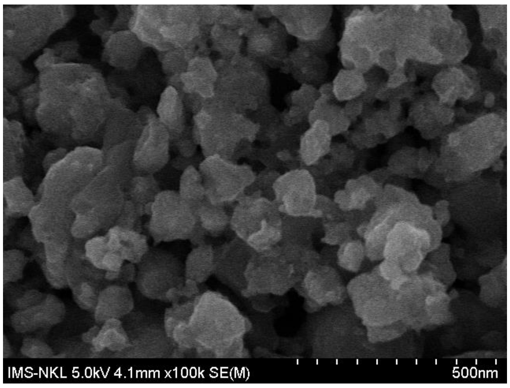

Fig. 3 High magnification SEM image of x=0.2 sample

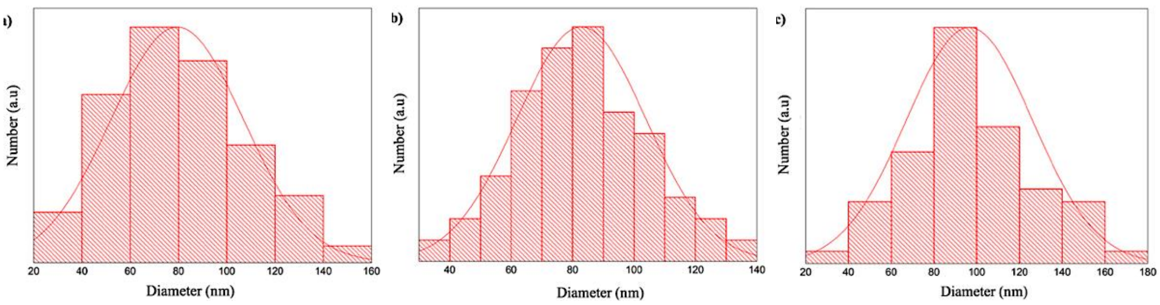

(a) x=0.1 (b) x=0.2 (c) x=0.3

Fig. 4 The particle sizes distribution of the as-milled $Cu_{2-x}ZnSnS_4$ powders after milling for 16 h with different compositions

milling for 16 h, and only XRD peaks of Cu_2ZnSnS_4 are formed at 2θ of 28.64, 32.9, 47.66, and 56.42°, which can be indexed to the planes of (112), (200), (220), and (312). It means that the structure of Cu_2ZnSnS_4 was formed and stable with the subtraction of Cu atoms in the crystal structure as x=0.1, 0.2, 0.3. It also can observe that the intensity of XRD peaks of $Cu_{2-x}ZnSnS_4$ decrease with the increase of x. This indicates that the distortion of crystal structure of $Cu_{2-x}ZnSnS_4$ increases with the reduction of Cu. The appearance of XRD patterns of the milled $Cu_{2-x}ZnSnS_4$ (x=0.1, 0.2, 0.3) powders were in a good agreement with previous researches, which used a similar

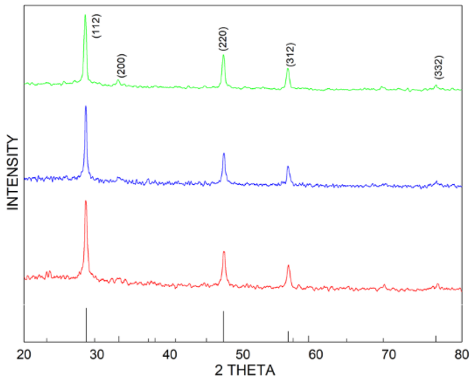

Fig. 5 XRD patterns of the heat-treated $Cu_{2-x}ZnSnS_4$ (*x*=0.1, 0.2, 0.3) powder samples

synthesis method (Long *et al.* 2020, Zhou *et al.* 2016).

The formation of $Cu_{2-x}ZnSnS_4$ (*x*=0.1, 0.2, 0.3) samples during high-energy ball mill was promoted by the diffusion process. During milling, the mixture of powders experienced heavy plastic deformation due to the ball collisions under the high milling speed. Subsequently, a large energy was transferred from balls collision to powders, which is able to activate the diffusion and reaction process of the powders without the need of heat-treatment. It known that the repeated processes of cold-welding and fracturing of powder particles resulted in a short distance and homogeneous diffusion of atoms. Besides, the fracturing of powder particles always creates new and clean surfaces for fast diffusion. Other factors including the formation of dislocations, vacancies, stacking faults, and temperature raise during milling further aids the diffusion process (Long *et al.* 2020, Kumar *et al.* 2017, Long *et al.* 2010, Suryanarayana 2001).

3.2 Morphology and particle sizes

Morphologies of the milled $Cu_{2-x}ZnSnS_4$ (*x*=0.1, 0.2, 0.3) powder samples were observed by FE-SEM. After milling for 16 h, the milled powders were formed with ultra-fine particles (Fig. 2). However, it can also be observed that the milled powders were agglomerated into large particles. This was explained that ultra-fine milled particles have the tendency to stick together (Long *et al.* 2010, Suryanarayana 2001). For a better understanding of the morphologies of milled powders, Fig. 3 provides a closer observation of individual milled powder particles displayed by a high magnification SEM image of *x*=0.2 sample.

The particle sizes of the milled $Cu_{2-x}ZnSnS_4$ (*x*=0.1, 0.2, 0.3) powders were estimated using ImageJ software, as shown in Fig. 4. In general, it can be seen that the distribution of particle sizes is varied in nanoscales. In particular, the particle sizes of *x*=0.1, 0.2 and 0.3 powder samples were mainly distributed in the ranges of 60-100, 70-90, and 80-100 nm, respectively.

3.3 Heat-treatment of the milled $Cu_{2-x}ZnSnS_4$ powders

The milled $Cu_{2-x}ZnSnS_4$ (*x*=0.1, 0.2, 0.3) powders were heat-treated at 723 K for 24 h to remove strain and improve the crystallinity before carrying out spark plasma sintering (SPS).

The XRD patterns of the heat-treated $Cu_{2-x}ZnSnS_4$ powders is shown in Fig. 5, revealed the presences of $Cu_{2-x}ZnSnS_4$ phase, which can be indexed to planes of (112), (200), (220), (312) and

Table 1 Lattice constants of $Cu_{2-x}ZnSnS_4$ (x=0, 0.1, 0.2, 0.3) samples

Composition	a (Å)	c (Å)	Reference
Cu_2ZnSnS_4	5.435	10.869	Long *et al.* 2020
$Cu_{1.9}ZnSnS_4$	5.434	10.898	This present work
$Cu_{1.8}ZnSnS_4$	5.423	10.868	This present work
$Cu_{1.7}ZnSnS_4$	5.421	10.852	This present work

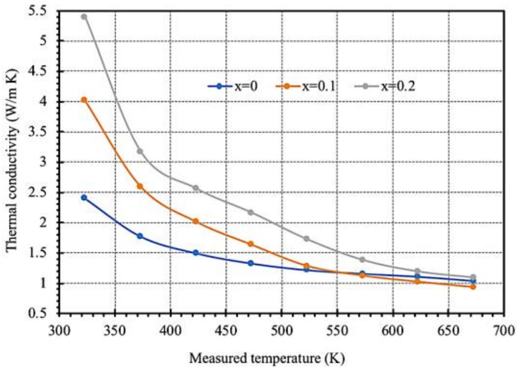

Fig. 6 Thermal conductivity of sintered $Cu_{2-x}ZnSnS_4$ (x=0, 0.1, 0.2) samples

(332). The XRD peaks of the heat-treated $Cu_{2-x}ZnSnS_4$ powders became sharp and high intensity compared to the non-heat-treatment powders, which could be attributed to the removement of strain, the increase of crystallite size and grain growth after heat-treatment.

The lattice constants of the heat-treated $Cu_{2-x}ZnSnS_4$ (x=0.1, 0.2, 0.3) powders were calculated based on the XRD results and given in Table 1. It can be seen that the lattice constants of a and c slightly decrease with the increase of x. The decrease of lattice constants can be explained due to the creation of vacancies at Cu sites (Nagaoka *et al.* 2018). The increase of x can lead to the increase of distortion degree of the crystal structure of $Cu_{2-x}ZnSnS_4$, which subsequently impacts on the thermal conductivity of the material (Long *et al.* 2021, Liu *et al.* 2009).

3.4 Thermal conductivity of $Cu_{2-x}ZnSnS_4$

The thermal conductivity $\kappa(T)$ of the sintered $Cu_{2-x}ZnSnS_4$ (x=0, 0.1, 0.2) samples is shown in Fig. 6. It is clear that the thermal conductivity of all samples decreased with the increase of temperature. Since heat is conducted in solid materials by the migration of free electrons and lattice vibration (phonon), the total thermal conductivity of solids can be expressed as (Tritt 2004, Abu-Eishah 2000, Long *et al.* 2021)

$$\kappa = \kappa_l + \kappa_e \tag{2}$$

where κ_l is the thermal conductivity due to phonons and κ_e is due to the migration of free electrons. Thus, with the increase of temperature, the vibration of atoms increases, which leads to the decrease of phonon mean free path, λ, the increase of electrons scattering and the electron-phonon interaction, which result in the decrease of thermal conductivity.

At temperatures below 600 K, the thermal conductivity of x=0 sample shows the lowest value compared to others in the measured temperature range. However, at temperatures above 600 K, the thermal conductivity of x=0.1 sample showes the lowest value in the measured range, in particularly κ=0.93 W/m K at 673 K. Compared to other researches, the thermal conductivity of x=0.1 sample is lower than that of Cu_2ZnSnS_4 (1.21 W/m K at 700 K), $Cu_{2.1}Zn_{0.9}SnS_4$ (1.12 W/m K at 700 K) (Liu *et al.* 2009), and similar to that of nano Cu_2ZnSnS_4 (0.97 W/m K at 700 K) (Yang *et al.* 2012). The low thermal conductivity of $Cu_{2-x}ZnSnS_4$ samples can be attributed to the ultra-fine grain size, crystal distortion and vacancy defects due to the decrease of the Cu content (Tritt, 2004, Liu *et al.* 2009, Fitriani *et al.* 2016, Zhang *et al.* 2016, Long *et al.* 2021). The fine grain size creates high specific volume of grain boundary, which leads to increase the phonon scattering and the reduction of carriers movement. While a partial subtraction of Cu atoms from the crystal structure could lead to increase the point defects and structure distortion scattering.

4. Conclusions

$Cu_{2-x}ZnSnS_4$ (x=0.1, 0.2, 0.3) samples were successfully synthesized by the solid-state reaction at the room temperature using the mechanical alloying method from the mixture of Cu, Zn, Sn and S powders. The synthesis method was able to prevent the evaporation of S. Ultra-fine milled $Cu_{2-x}ZnSnS_4$ powders were obtained after 16 h of milling, which mostly distributed in the range of 60 to 100 nm. The milled powder particles tended to agglomerate into large particles. The lattice constants of *a* and *c,* and thermal conductivity decreased with the subtraction of Cu atoms from the crystal structure. The thermal conductivity of x=0.1 sample exhibited a minimum value of 0.93 W/m K at 673 K.

Acknowledgments

This research is funded by Hanoi University of Science and Engineering (HUST) under project number T2022-PC-082.

References

Abu-Eishah, S.I. (2000), "Correlations for the thermal conductivity of metals as a function of temperature", *Int. J. Thermophys.*, **22**, 1855-1868. https://doi.org/10.1023/A:1013155404019.

Fitriani, R.O., Long, B.D., Barma, M.C., Riaz, M., Sabri, M.F.M., Said, S.M. and Saidur, R. (2016), "A review on nanostructures of high-temperature thermoelectric materials for waste heat recovery", *Renewab. Sustainab. Energy Rev.*, **64**, 635-659. http://doi.org/10.1016/j.rser.2016.06.035.

Freer, R. and Powell, A.V. (2020), "Realising the potential of thermoelectric technology: A roadmap", *J. Mater. Chem. C*, **8**, 441-463. https://doi.org/10.1039/C9TC05710B.

Ge, Z.H., Zhao, L.D., Wu, D., Liu, X., Zhang, B.P., Li, J.F. and He, J. (2016), "Low-cost, abundant binary sulfides as promising thermoelectricmaterials", *Mater. Today*, **19**(4), 227-239. http://doi.org/10.1016/j.mattod.2015.10.004.

Jaziri, N., Boughamoura, A., Müller, J., Mezghani, B., Tounsi, F. and Ismail, M. (2020), "A comprehensive review of thermoelectric generators: Technologies and common applications", *Energy Rep.*, **6**, 264-287. https://doi.org/10.1016/j.egyr.2019.12.011.

Jiang, Q., Yan, H., Lin, Y., Shen, Y., Yang, J. and Reece, M.J. (2020), "Colossal thermoelectric enhancement in $Cu_{2+x}Zn_{1-x}SnS_4$ solid solution by local disordering of crystal lattice and multi-scale defect engineering", *J. Mater. Chem. A*, **8**, 10909-10916. https://doi.org/10.1039/D0TA01595D.

Kosuga, A., Matsuzawa, M., Hories, A., Omoto, T. and Funahashi, R. (2015), "High-temperature thermoelectric properties and thermal stability in air of copper zinc tin sulfide for the p-type leg of thermoelectric devices", *Japan. J. Appl. Phys.*, **54**, 061801. http://doi.org/10.7567/JJAP.54.061801.

Kumar, A., Pandel, U. and Banerjee, M.K. (2017), "Effect of high energy ball milling on the structure of iron - multiwall carbon nanotubes (MWCNT) composite", *Adv. Mater. Res.*, **6**(3), 245-255. https://doi.org/10.12989/amr.2017.6.3.245.

Liu, M.L., Huang, F.Q., Chen, L.D. and Chen, I.W. (2009), "A wide-band-gap p-type thermoelectric material based on quaternary chalcogenides of Cu_2ZnSnQ_4 (Q=S,Se…)", *Appl. Phys. Lett.*, **94**, 202103. https://doi.org/10.1063/1.3130718.

Long, B.D., Khanh, N.V., Binh, D.N. and Hai, N.H. (2020), "Thermoelectric properties of quaternary chalcogenide Cu_2ZnSnS_4 synthesised by mechanical alloying", *Powder Metall.*, **63**(3), 220-226. https://doi.org/10.1080/00325899.2020.1783103.

Long, B.D., Khanh, N.V., Binh, D.N., Thang, L.H., Bang, L.T and Said, S.B.M. (2019), "Synthesis of Cu_2ZnSnS_4 by mechanical alloying method for thermoelectric application", *Acta Metall. Slovaca*, **25**(3), 174-179. https://doi.org/10.12776/ams.v25i3.1311.

Long, B.D., Thang, L.H., Hai, N.H., Suekuni, K., Hashikuni, K., Nhat, T.Q.M., Klich, W. and Ohtaki, M. (2021), "Thermoelectric quaternary sulfide $Cu_{2+x}Zn_{1-x}SnS_4$ (x=0-0.3): Effects of Cu substitution for Zn", *Mater. Sci. Eng. B*, **272**, 115353. https://doi.org/10.1016/j.mseb.2021.115353.

Long, B.D., Zuhailawati, H., Umemoto, M., Todaka, Y. and Othman, R. (2010), "Effect of ethanol on the formation and properties of a Cu-NbC composite", *J. Alloys Compd.*, **503**, 228-232. https://doi.org/10.1016/j.jallcom.2010.04.243.

Nagaoka, A., Masuda, T., Yasui, S., Taniyama, T. and Nose, Y. (2018), "The single-crystal multinary compound Cu_2ZnSnS_4 as an environmentally friendly high-performance thermoelectric material", *Appl. Phys. Exp.*, **11**, 051203. https://doi.org/10.7567/APEX.11.051203.

Row, D.M. (2012), *Thermoelectrics and Its Energy Harvesting: Modules, Systems, and Applications in Thermoelectrics*, CRC Press, Boca Raton, FL, USA.

Suryanarayana, C. (2001), "Mechanical alloying and milling", *Prog. Mater. Sci.*, **46**, 1-184. https://doi.org/10.1016/S0079-6425(99)00010-9.

Tritt, T.M. (2004), *Thermal Conductivity: Theory, Properties, and Application*, Kluwer Academic/Plenum Publishers, New York, NY, USA.

Yang, H., Jauregui, L.A., Zhang, G., Chen, Y.P. and Wu, Y. (2012), "Nontoxic and abundant copper zinc tin sulfide nanocrystals for potential high-temperature thermoelectric energy harvesting", *Nano Lett.*, **12**, 540-545. https://doi.org/10.1021/nl201718z.

Zhang, D., Yang, J., Jiang, Q., Fu, L., Xiao, Y., Luo, Y. and Zhou, Z. (2016), "Improvement of thermoelectric properties of Cu_3SbSe_4 compound by In doping", *Mater. Des.*, **98**, 150-154. http://doi.org/10.1016/j.matdes.2016.03.001.

Zhou, Y., Xi, S., Sun, C. and Wu, H. (2016), "Facile synthesis of Cu_2ZnSnS_4 powders by mechanical alloying and annealing", *Mater. Lett.*, **169**, 176-179. http://doi.org/10.1016/j.matlet.2016.01.116.

CC